View metadata, citation and similar papers at core.ac.uk

brought to you by CORE

provided by Carolina Digital Repository

Concerted electron-proton transfer in the optical excitation of hydrogen-bonded dyes

Brittany C. Westlake, M. Kyle Brennaman, Javier J. Concepcion, Jared J. Paul, Stephanie E. Bettis, Shaun D. Hampton, Stephen A. Miller, Natalia V. Lebedeva, Malcolm D. E. Forbes, Andrew M. Moran, Thomas J. Meyer[1], and John M. Papanikolas[1]

Department of Chemistry, University of North Carolina at Chapel Hill, Chapel Hill, NC 27599

Contributed by Thomas J. Meyer, March 28, 2011 (sent for review February 10, 2011)

The simultaneous, concerted transfer of electrons and protons—electron-proton transfer (EPT)—is an important mechanism utilized in chemistry and biology to avoid high energy intermediates. There are many examples of thermally activated EPT in ground-state reactions and in excited states following photoexcitation and thermal relaxation. Here we report application of ultrafast excitation with absorption and Raman monitoring to detect a photochemically driven EPT process (photo-EPT). In this process, both electrons and protons are transferred during the absorption of a photon. Photo-EPT is induced by intramolecular charge-transfer (ICT) excitation of hydrogen-bonded-base adducts with either a coumarin dye or 4-nitro-4′-biphenylphenol. Femtosecond transient absorption spectral measurements following ICT excitation reveal the appearance of two spectroscopically distinct states having different dynamical signatures. One of these states corresponds to a conventional ICT excited state in which the transferring H^+ is initially associated with the proton donor. Proton transfer to the base (B) then occurs on the picosecond time scale. The other state is an ICT-EPT photoproduct. Upon excitation it forms initially in the nuclear configuration of the ground state by application of the Franck–Condon principle. However, due to the change in electronic configuration induced by the transition, excitation is accompanied by proton transfer with the protonated base formed with a highly elongated $^+$H—B bond. Coherent Raman spectroscopy confirms the presence of a vibrational mode corresponding to the protonated base in the optically prepared state.

electron transfer | proton-coupled electron transfer

Proton-coupled electron transfer (PCET), in which electrons and protons are both transferred, is at the heart of many energy conversion processes in chemistry and biology (1–6). PCET reactions can occur by sequential two-step transfers (e.g., electron transfer followed by proton transfer, ET-PT, or proton transfer followed by electron transfer, PT-ET) or by concerted electron-proton transfer (EPT) (1, 2). EPT pathways are important in avoiding high-energy intermediates, playing an integral role in photosynthesis and respiration, for example.

Photo-driven EPT (photo-EPT), with electron and proton transfers occurring simultaneously during the optical excitation process, would appear to be ruled out on fundamental grounds, because electronic excitation occurs rapidly on the time scale for nuclear motions, including proton transfer. Using a combination of femtosecond pump-probe and coherent Raman techniques, we have observed simultaneous electron-proton transfer induced by intramolecular charge transfer (ICT) excitation in two different hydrogen-bonded adducts formed between an organic dye (A—O—H) and an external base (:B). One is formed between a *para*-nitrophenyl-phenol and an amine base, and the other between a coumarin derivative and an imidazole base (Fig. 1).

The shift in electron density away from the hydroxyl group to the intramolecular acceptor during ICT excitation greatly enhances the acidity of the hydrogen-bonded proton and leads to proton transfer in the excited state (7–9). Initially, the proton in the optically prepared ICT excited state is located

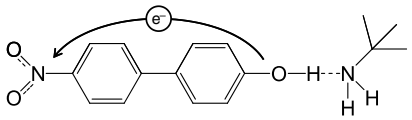

(1) Nitrophenyl-Phenol / t-Butylamine

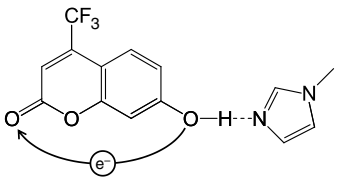

(2) Hydroxy-Coumarin / Methyl Imidazole

Fig. 1. Chemical structures of the two hydrogen-bonded adducts studied in this work: (1) 4-hydroxy-4′-nitro-biphenyl (para-nitrophenyl-phenol) and *t*-butylamine (TBA) in 1,2 dicholoro-ethane (DCE). Hydrogen bonding is confirmed for a range of bases in a variety of solvents using UV-visible and direct infrared absorption. (2) 7-hydroxy-4-(trifluoromethyl)-coumarin and 1-methylimidazole in toluene. Evidence of hydrogen-bonding in the ground state is observed by shifts in the coumarin absorption spectrum.

at the equilibrium coordinate of the A—O—H ground state, $(^{-\cdot}A—O^{\cdot}—H^+\cdots:B)^*$. In a conventional proton transfer event, H^+ motion occurs after excited state equilibration in coupled vibrational and solvent modes. The stepwise process is analogous to ET-PT with excitation (ET) followed by proton transfer and has been studied by several groups using ultrafast methods (9–12). Conversely, the same configuration produced by vertical excitation could also be viewed as an ICT-EPT photoproduct. In this product, the proton has transferred to the nitrogen in concert with the change in electronic configuration induced by the optical excitation. A protonated base is formed with a highly elongated $^+$H—N bond[†]—i.e., $(^{-\cdot}A—O^{\cdot}\cdots{}^+H—B)^*$ (Fig. 2). A predicted spectroscopic signature of such an "ICT-EPT" transition would be possible appearance of a second optically accessible excited state and the instantaneous appearance of an H^+—N vibrational mode.

Results and Discussion

We report here results on two systems in which ICT to an internal electron acceptor is accompanied by proton transfer to an

Author contributions: M.D.F., A.M.M., T.J.M., and J.M.P. designed research; B.C.W., M.K.B., J.J.C., J.J.P., S.E.B., S.D.H., S.A.M., and N.V.L. performed research; B.C.W., M.K.B., J.J.P., M.D.F., A.M.M., T.J.M., and J.M.P. analyzed data; and T.J.M. and J.M.P. wrote the paper.

The authors declare no conflict of interest.

See Commentary on page 8531.

[†]The femtosecond laser pulses used here most likely do not have the bandwidth to excite an H-N vibrational wavepacket. As a consequence, the excited state nuclear wavefunction probably extends to some degree across the ICT-EPT well.

[1]To whom correspondence may be addressed. E-mail: tjmeyer@unc.edu or John_Papanikolas@unc.edu.

This article contains supporting information online at www.pnas.org/lookup/suppl/doi:10.1073/pnas.1104811108/-/DCSupplemental.

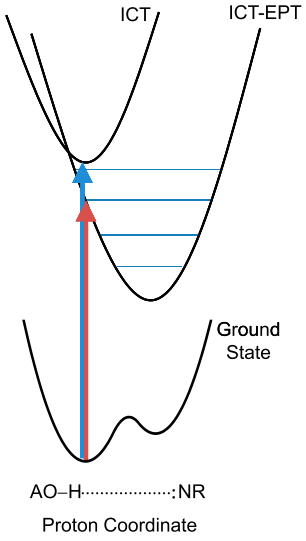

Fig. 2. Illustration of the ICT and ICT-EPT energy-coordinate surfaces. Red and blue arrows illustrate excitation wavelengths used in this work. Excitation of the ICT state (blue arrow) results in delayed proton transfer. Proton transfer occurs concomitantly with excitation to the ICT-EPT state (red arrow).

external base. Structures are shown in Fig. 1. In both cases, the hydroxyl group on the chromophore forms an intermolecular hydrogen bond with a nitrogen-containing base in solution—i.e., A—O—H···:B.

We present results first on the hydrogen-bonded adduct formed between *para*-nitrophenyl-phenol and *t*-butylamine (**1**) in 1,2-dichloroethane (DCE). Spectroscopic measurements (IR, UV visible) demonstrate hydrogen-bond formation in the ground state—i.e., A—O—H···:B. Femtosecond transient absorption experiments performed at different excitation wavelengths on the hydrogen-bonded adduct reveal two optically accessible states that produce different photoproducts. In one, the H-bonded proton is still associated with the oxygen atom. In the other, it is bound to the base but, by application of the Franck–Condon principle, through an elongated H^+—N bond. Coherent Raman spectra of the optically prepared state obtained at the moment of excitation show the appearance of a $\nu(H^+—N)$ mode at higher frequency, consistent with transfer of the proton to the base during the ICT excitation process. A similar feature is observed in ultrafast Raman spectra of the hydrogen-bonded adduct formed between hydroxy-coumarin and 1-methyl-imidazole (**2**) in toluene.

***Para*-nitrophenyl-phenol.** ICT absorption in *para*-nitrophenyl-phenol promotes an electron from a nonbonding orbital on the oxygen to the nitro group, producing a $^1(n\pi^*)$ charge transfer excited state (Fig. 1).

Analysis of ground-state absorption spectra for a series of organic bases shows that the ICT absorption band at 335 nm systematically shifts to lower energy as the O—H bond is weakened through hydrogen bonding, ultimately leading to deprotonation. Hydrogen-bond formation with bases ranging from *t*-butylamine ($pK_a = 10.7$) to pyridine ($pK_a = 5.25$) in DCE result in incremental shifts in the ICT absorption band with increasing base strength from $\lambda_{max} = 335$ nm (no base) to a limiting value of 354 nm for *t*-butylamine. For *t*-butylamine, $K_A = 104 \pm 10\ M^{-1}$ at 23 ± 2 °C with adduct formation >90% complete with 0.3 mM *para*-nitrophenyl phenol and 90 mM base. The latter were the experimental conditions used in the transient experiments.

Complete deprotonation of the phenol occurs upon addition of tetra-*n*-butylammonium hydroxide, which further red shifts the ICT absorption to $\lambda_{max} = 466$ nm. The intermediate proton transfer state, A—O^-···H^+—:B, cannot be accessed experimentally; however, DFT calculations suggest that its ICT absorption lies at 410 nm between the absorptions for the hydrogen-bonded (354 nm) and deprotonated forms of the phenol (466 nm). The position of the ICT absorption provides a spectroscopic indicator of the location of the proton in the ground state, ranging from 335 nm (A—O—H) to 354 nm (A—O—H···:B) to 410 nm (A—O^-···$^+$H—B) to 466 nm (A—O^-). Examination of the ground-state absorption spectrum (Section I.B, *SI Appendix*) shows no evidence of significant concentrations of either deprotonated anion (A—O^-) or proton transfer adduct (A—O^-···$^+$H—B). These observations are consistent with both states lying energetically above the hydrogen-bonded adduct.

The acidity in the ICT excited state is enhanced by approximately 9 pK_a units, resulting in a large driving force for proton transfer after photoexcitation. We have used a combination of femtosecond transient absorption and coherent Raman spectroscopies to probe the structure of the optically prepared state and the dynamics that take place following photon absorption. Details regarding observations and analysis can be found in Sections I.C and III of the *SI Appendix*.

Femtosecond transient absorption spectra of the hydrogen-bonded adduct show evidence for three excited state absorption bands between 400 and 700 nm. The spectra obtained one picosecond following excitation of the free *para*-nitrophenyl-phenol and the hydrogen-bonded adduct (**1**) are shown in Fig. 3.

Excitation of free phenol at 355 nm in DCE results in an absorption band with $^1\lambda_{max} = 440$ nm (labeled S_a in Fig. 3). It is assigned to an excited state absorption from the singlet $^1n\pi^*$ ICT state—i.e., $^1(^{-\cdot}A—O^{\cdot}—H^+)^*$. The singlet undergoes rapid ($\tau \sim 3$ ps) intersystem crossing to the corresponding $^3n\pi^*$ state, $^1(^{-\cdot}A—O^{\cdot}—H^+)^* \rightarrow {}^3(^{-\cdot}A—O^{\cdot}—H^+)^*$, giving rise to the red absorption band at $^3\lambda_{max} = 630$ nm, denoted T_a. The triplet character of the red absorption was verified by transient EPR measurements at 77 K in a toluene glass (*SI Appendix*) and the intersystem crossing time observed here is comparable to that observed for $n\pi^*$ states in nitrobenzenes (13). The T_a band reaches its maximum amplitude within a few ps and then decays, without a change in spectral position on a time scale of 2–3 μs.

The singlet and triplet bands are also observed in the transient absorption spectra of the hydrogen-bonded adduct (A—O—H···:B), Fig. 3. These absorptions depend upon excitation wavelength and exhibit complex temporal evolution including changes in both the amplitude and position of the bands. Our analysis of the transient spectra, which is discussed in detail in the *SI Appendix*, correlates observations of the spectral evolution from fs to μs, at two different excitation wavelengths, 355 nm and 388 nm.

The singlet and triplet absorptions observed following 388 nm excitation of the adduct (S_c and T_c) are both shifted to higher energy relative to the free phenol, with λ_{max} at 395 nm and 570 nm, respectively. While the singlet absorption decays with $\tau \sim 4.5$ ps, the triplet absorption shows no appreciable evolution during the first 300 ps after excitation.

With 355 nm excitation, the singlet band is shifted to higher energy relative to the unassociated phenol with λ_{max} at 410 nm (Fig. 3). The triplet band appears at $\lambda_{max} = 620$ nm at early pump-probe delays, similar to the phenol itself (Section I.C.1, *SI Appendix*).

Careful examination of the singlet absorption reveals that the red and blue edges decay with different kinetics, consistent with two unresolved absorptions with different decay characteristics (Section 1.C.2, *SI Appendix*). The decay on the lower-energy side is kinetically correlated with the growth of the triplet absorption at 630 nm ($\tau \sim 1.5$ ps), a clear indication that it arises from the singlet ICT state, $^1(^{-\cdot}A—O^{\cdot}—H^+\cdots:B)^*$. The higher-energy side decays more slowly with $\tau \sim 4.5$ ps. This is identical to the lifetime

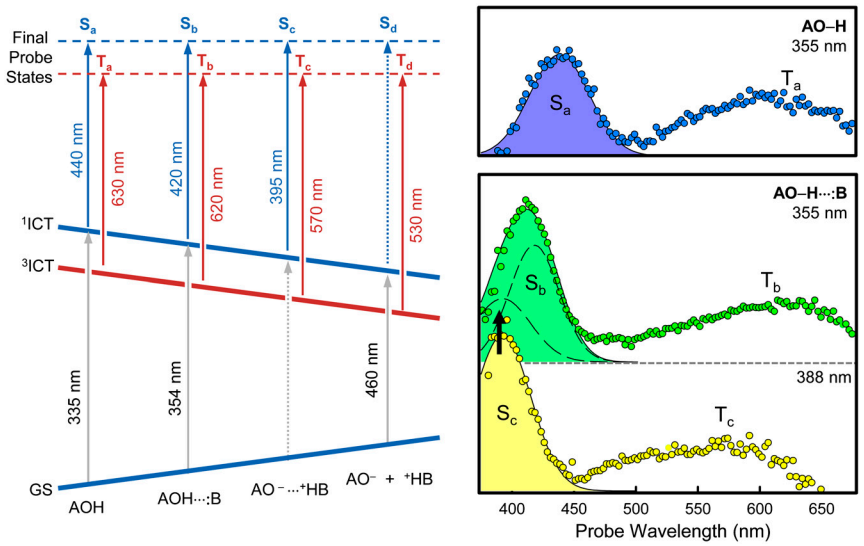

Fig. 3. Transient absorption spectra at early pump-probe delay times of 4-hydroxy-4′-nitro-biphenyl (nitrophenyl-phenol) (*Upper*, right) and the hydrogen-bonded adduct with *t*-butylamine (TBA) (*Lower*, right) in 1,2 dicholoro-ethane (DCE). All spectra were observed 1.0 ps after photoexcitation. The free phenol spectrum was obtained after photoexcitation at 355 nm. Two spectra for the hydrogen-bonded adduct are shown, collected at 355 nm and the other at 388 nm. The diagram at the left illustrates the band assignments made by correlation of a wide array of experimental observations (see *SI Appendix*). The dashed gray and blue arrows indicate transitions that are not observed experimentally.

of S_c, suggesting that it and the unresolved higher-energy contribution in the 355 nm spectrum arise from the same transition. Taking this contribution to have the same position and spectral width as S_c enables a deconvolution of the two unresolved absorptions and suggests that the lower-energy absorption (S_b) has its λ_{max} at 420 nm. These two bands (S_b and S_c) are depicted by the dashed lines beneath the singlet absorption band in the 355 nm spectrum.

The shift of the singlet absorption from 440 nm in free *para*-nitrophenyl-phenol (S_a) to 420 nm when hydrogen bonded to the amine (S_b) indicates that the excited state absorption in the ICT state is also sensitive to the location of the proton, shifting to the blue as the O—H bond weakens. With this observation the appearance of the feature at $\lambda_{max} \approx 395$ nm is consistent with a $^1n\pi^*$ ICT state that has a considerable degree of proton transfer character—i.e., $^1(^{-\cdot}A—O^{\cdot}\cdots{}^+H—B)^*$. The proton in this configuration is located at the same nuclear configuration as in the ground state, by application of the Frank–Condon approximation, but is transferred to the base.

This systematic blue shift with O—H bond weakening is also observed in the triplet absorption. Peaking at 630 nm in the free phenol, $^3(^{-\cdot}A—O^{\cdot}—H^+)^*$, this band is observed to shift to higher energy as the interaction with the proton is weakened, first through hydrogen bonding $^3(^{-\cdot}A—O^{\cdot}—H^+\cdots:B)^*$, 620 nm, then proton transfer to the base $^3(^{-\cdot}A—O^{\cdot}\cdots{}^+H—B)^*$, 570 nm, and ultimately with deprotonation to the anion $^3(^{-\cdot}A—O^{\cdot})^*$, 530 nm (Section I.C.2, *SI Appendix*). The transition energies of the ground and excited state absorptions for the different protonation states of the nitrophenyl-phenol chromophore are summarized schematically in Fig. 3.

Based on our band assignments, the transient spectra at early times suggest that there are two spectroscopically accessible states corresponding to the configurations $^1(^{-\cdot}A—O^{\cdot}—H^+\cdots:B)^*$ and $^1(^{-\cdot}A—O^{\cdot}\cdots{}^+H—B)^*$. They are illustrated in the energy-coordinate diagram shown in Fig. 2. While both states appear to be populated by 355 nm excitation (as evidenced by the presence of both S_b and S_c), 388 nm excitation seems to produce only the latter. The absence of the $^1(^{-\cdot}A—O^{\cdot}—H^+\cdots:B)^*$ absorption feature following 388 nm excitation suggests that, at the ground-state geometry, $^1(^{-\cdot}A—O^{\cdot}\cdots{}^+H—B)^*$ is lowest in energy, as depicted in the figure. It is interesting to note that similar ultrafast proton transfer has been observed in related measurements on the green fluorescent protein (GFP). In GFP ultrafast proton transfer was attributed to excitation to a second state underlying the electronic absorption band, but the nature of the transition was unclear (10).

In the *para*-nitrophenyl-phenol adduct, the two initial singlet states have distinctly different dynamical signatures. Photoexcitation to $^1(^{-\cdot}A—O^{\cdot}—H^+\cdots:B)^*$ results in delayed proton transfer following intersystem crossing to the triplet, $^3(^{-\cdot}A—O^{\cdot}—H^+\cdots:B)^*$. Excitation to the lower-energy surface at 388 nm gives rise to prompt appearance of protonated base—i.e., $(^{-\cdot}A—O^{\cdot}\cdots{}^+H—B)^*$ in both the singlet and triplet spectra.

The presence of $(^{-\cdot}A—O^{\cdot}\cdots{}^+H—B)^*$ at the earliest observable pump-probe delay times (200 fs) is consistent with a photoinduced electron-proton transfer (photo-EPT) process. However, given the time scale of the experiment, we cannot rule out the presence of an ultrafast but delayed proton transfer process that occurs during the 200 fs excitation pulse solely from the transient absorption data. The key question is whether direct photoexcitation to the ICT-EPT state occurs from the ground-state configuration.

Coherent Raman measurements provide a direct probe of excited state vibrational modes at the Franck–Condon geometry. Similar to spontaneous resonance Raman spectroscopy, the amplitudes of the vibrational resonances reflect geometric distortions between the ground and excited states (i.e., Franck–Condon factors). However, application of a broadband field initiates nuclear motion on both the ground and excited state surfaces.

Details involved in the acquisition and analysis of the Raman signals are provided in the *SI Appendix*. A typical coherent Raman spectrum obtained from the *para*-nitrophenyl-phenol adduct is shown in Fig. 4. In this representation, the spectra contain positive and negative going signals, which are described for a general system by Eq. **S8** in the *SI Appendix*. For the systems discussed here, the signals with positive signs correspond to nuclear coherences in the ground electronic state, while the negative going signals are associated with nuclear coherences in the excited electronic state.

The spectrum of the nitrophenyl-phenol adduct shows the ν(O—H) ground-state band at 2,850 cm^{-1} and a band at 2,970 cm^{-1} that is assigned to an excited state vibrational coher-

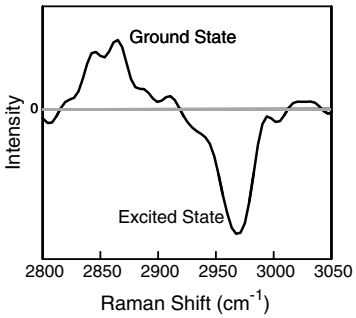

Fig. 4. Coherent Raman spectrum of the nitrophenyl-phenol/t-butylamine hydrogen-bonded adduct. The positive going feature is the Raman response of the O—H mode in the ground electronic state. The higher frequency negative going feature is an excited state vibrational resonance assigned to the $^{+}$H—N mode.

ence based on the sign of the signal. ICT excitation of the *para*-nitrophenyl-phenol weakens the O—H bond and shifts its vibrational frequency to lower energy, suggesting that the O—H mode is not the origin of the excited state resonance. Based on the shift to higher energy, the new band is assigned to the ν(N—H^{+}) mode in the ICT adduct. The 2,970 cm^{-1} frequency is consistent with ν(N—H^{+}) stretching vibrations observed in protonated amines (14), which range from 3,100 to 3,300 cm^{-1}.

From a Frank–Condon perspective, excitation to the ICT-EPT state is a vertical process along the coupled nuclear coordinates including the proton transfer coordinate. The formation of the protonated base in the optical excitation process is remarkable because it implies that there is redistribution of electron density both in the phenol and at the base. The rearrangement of electron density in intramolecular examples is expected because both the proton donor and acceptor are part of the same electronic framework. The electronic redistribution at the base in the intermolecular adduct is noteworthy, pointing to extensive electronic coupling across the hydrogen bond.

Hydroxy-Coumarin. ICT excitation of 7-hydroxy-4-(tri-fluoromethyl)-coumarin (HFC) promotes a largely nonbonding electron from the hydroxyl group to a π^{*} orbital with considerable carbonyl character, increasing the acidity of the OH proton by approximately 14 pK_a units (7, 8). Evidence of ground-state H-bonding between the coumarin and 1-methyl-imidazole (1-MeIm) base in toluene is observed as a shift in the ICT absorption spectrum from 330 nm to 342 nm upon adduct formation. For 1-methylimidazole, $K_A = 2{,}100$ M^{-1} with adduct formation of 73% at 2 mM base concentration.

We have used the emissive properties of the coumarin to probe coupled electron-proton transfer following ultrafast excitation. In the absence of an external base, hydroxy-coumarins emit weakly with an emission maximum in toluene of 403 nm. The deprotonated form is strongly emissive with $\lambda_{max} = 506$ nm. Intense emission is also observed upon the addition of hydrogen-bonding bases, and the 1:1 adduct with 1-MeIm (A—O—H···:B) emits at 459 nm (15). The blue-shifted emission in the adduct relative to the anion can be attributed to H-bond stabilization of the ground-state anion by complex formation with the protonated base.

The appearance of the emission at 459 nm is thus an indicator of proton transfer in the excited state. Femtosecond transient absorption methods were used to monitor the growth of stimulated emission at 459 nm (Fig. 5*A*). Based on this result, approximately 75% of the emission appears on a time scale short relative to the instrument response time (<1 ps) consistent with rapid proton transfer.

The coherent Raman spectrum for the coumarin adduct is shown in Fig. 5*B*. Like *para*-nitrophenyl-phenol, the ν(O—H)

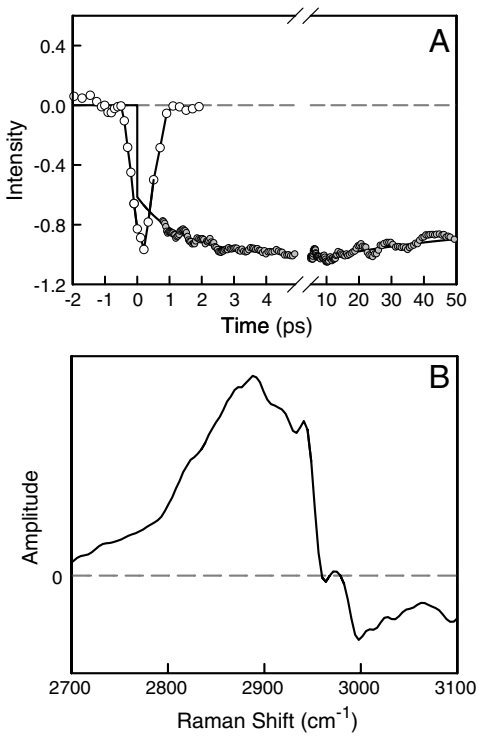

Fig. 5. (*A*) Transient stimulated emission data for the hydroxyl-coumarin 1:1 adduct with 1-MeIm (2 mM) in toluene following 355 nm excitation. The open circles display the laser excitation pulse reacting with the solvent nuclear response in toluene. Gray points represent the stimulated emission data at 465 nm; only data points outside the instrument response are shown. (*B*) Coherent Raman spectrum of the hydroxyl coumarin 1:1 adduct with 1-MeIm (2 mM) in toluene.

Raman response of the ground state is observed at 2,900 cm^{-1}, whereas an excited state vibrational resonance is observed near 3,050 cm^{-1}. Based on the shift to higher energy, the new band can be assigned to ν(N—H^{+}) in the ICT adduct ^{1}($^{-\cdot}$A—O$^{\cdot}$···$^{+}$H—B)*.

Conclusions

Our spectroscopic results reveal the presence of a concerted electron-proton transfer process in the optical ICT excitation of two different hydrogen-bonded dyes. Transient absorption spectra reveal that two spectroscopic states are accessed having different dynamical signatures. One of the states corresponds to a conventional excited state proton transfer process in which proton transfer occurs after vibrational and solvent relaxation. The other is an ultrafast concerted electron-proton transfer event with proton transfer coupled to the change in electronic configuration. The appearance of the ν(N—H^{+}) mode in the coherent Raman spectra shows that the proton transfer state is directly accessible via optical excitation. Here charge transfer occurs in concert with proton transfer to the nitrogen atom of the acceptor base with the newly formed H—N bond highly elongated along the H—N axis, ($^{-\cdot}$A—O$^{\cdot}$···$^{+}$H—B)*, as illustrated in Fig. 2. The evidence points to concerted transitions in both cases in which a proton transfer state is formed directly from the ground state during the ICT excitation.

Experimental Methods

A brief description of the materials and experimental methods are provided below and more detail can be found in the *SI Appendix*.

Materials. 4-hydroxy-4′-nitrobiphenyl (nitrophenyl-phenol) was purchased from TCI America and used as received. 7-hydroxy-

4-(trifluoromethyl)-1-coumarin (coumarin) (98%), and 1-methylimidazole (1-MeId) (99%) were purchased from Sigma-Aldrich and used as received. All solvents were purchased from Aldrich and used as received. All experiments on *para*-nitrophenyl-phenol were performed in dichloro-ethane (DCE). All experiments on the coumarin dye were performed in toluene.

Femtosecond Transient Absorption. Femtosecond transient absorption measurements were done using a pump-probe technique based on a Ti:Sapphire chirped pulse amplification (CPA) laser system (Clark-MXR CPA-2001). The pump pulse was produced by an Optical Parametric Amplifier (OPA) and the probe pulse was generated by continuum generation in a CaF_2 substrate and detected by a CCD camera. The spectrometer is capable of measuring transient spectra with approximately 200 fs time resolution and a sensitivity of better than 1 mOD.

Nanosecond Transient Absorption. The nanosecond transient absorption spectrometer is based on a Nd:YAG/OPO laser system used for sample excitation. The transient changes in a white-light continuum generated by Xe arc lamp were detected by a monochromator/PMT system and monitored using a digital oscilloscope.

Coherent Raman Spectrometer. The coherent Raman experiments apply two narrowband pulses and two broadband pulses with independently controlled delays; one broadband pulse is used for signal detection by spectral interferometry. The narrowband pulses are 500 fs in duration with spectra centered at 400 nm. The 355 nm broadband pulses have durations of 45 fs. The pulses are focused to 120 um FWHM spot size at the sample and possess energies of 50–100 nJ. Signals are detected using a back-illuminated CCD array (Princeton Instruments PIXIS 100B) mounted on a 0.3 m spectrograph.

ACKNOWLEDGMENTS. Support by National Science Foundation Grants CHE0957215 (T.J.M.), CHE0809530 (M.D.E.F.), and CHE0809045 (J.M.P.) is gratefully acknowledged. In addition, support for S.A.M., and support for B.C.W and M.K.B during the latter stages of the project, was provided as part of University of North Carolina Solar Fuels and Next Generation Photovoltaics, an Energy Frontier Research Center funded by the US Department of Energy, Office of Science, Office of Basic Energy Sciences under Award DE-SC0001011.

1. Huynh M, Meyer T (2007) Proton-coupled electron transfer. *Chem Rev* 5004–5064.
2. Gagliardi CJ, et al. (2010) Integrating proton coupled electron transfer (PCET) and excited states. *Coord Chem Rev* 254:2459–2471.
3. Hammes-Schiffer S, Iordanova N (2004) Theoretical studies of proton-coupled electron transfer reactions. *Biochim Biophys Acta* 1655:29–36.
4. Hammes-Schiffer S (2009) Theory of proton-coupled electron transfer in energy conversion processes. *Acc Chem Res* 42:1881–1889.
5. Meyer T, Huynh M, Thorp H (2007) The possible role of proton-coupled electron transfer (PCET) in water oxidation by photosystem II. *Angew Chem Int Ed Engl* 46:5284–5304.
6. Chang CJ, Chang MCY, Damrauer NH, Nocera DG (2004) Proton-coupled electron transfer: A unifying mechanism for biological charge transport, amino acid radical initiation and propagation, and bond making/breaking reactions of water and oxygen. *Biochim Biophys Acta* 1655:13–28.
7. Cohen B, Huppert D (2001) Evidence for a continuous transition from nonadiabatic to adiabatic proton transfer dynamics in protic liquids. *J Phys Chem A* 105:2980–2988.
8. Cohen B, Huppert D (2001) Excited state proton-transfer reactions of coumarin 4 in protic solvents. *J Phys Chem A* 105:7157–7164.
9. Tolbert L, Solntsev K (2002) Excited-state proton transfer: From constrained systems to "super" photoacids to superfast proton transfer. *Acc Chem Res* 35:19–27.
10. Shi X, et al. (2007) Ultrafast excited-state dynamics in the green fluorescent protein variant S65T/H148D. 2. Unusual photophysical properties. *Biochemistry* 46:12014–12025.
11. Shu X, et al. (2007) Ultrafast excited-state dynamics in the green fluorescent protein variant S65T/H148D. 1. Mutagenesis and structural studies. *Biochemistry* 46:12005–12013.
12. Leiderman P, et al. (2007) Ultrafast excited-state dynamics in the green fluorescent protein variant S65T/H148D. 3. Short- and long-time dynamics of the excited-state proton transfer. *Biochemistry* 46:12026–12036.
13. Yip R, Sharma D, Giasson R, Gravel D (1984) Picosecond excited-state absorption of alkyl nitrobenzenes in solution. *J Phys Chem* 88:5770–5772.
14. Socrates G (2001) *Infrared and Raman Characteristic Group Frequencies* (Wiley, New York), 3rd Ed.
15. Shank CV, Dienes A, Trozzolo AM, Myer JA (1970) Near UV to yellow tunable laser emission from an organic dye. *Appl Phys Lett* 16:405–407.